Electrostatic effects of nanoscale dielectric patches in the modification of Schottky contacts

Justin C. W. Song, Kuan Eng J. Goh,* Natarajan Chandrasekhar, and Cedric Troadec
*Institute of Materials Research and Engineering, Agency for Science, Technology and Research (A*STAR), 3 Research Link, Singapore 117 602, Singapore*

(Received 2 February 2009; revised manuscript received 13 March 2009; published 17 April 2009)

We study the electrostatic effects of thin organic films in modifying the interface physics of metal/semiconductor Schottky contacts. We work out analytically the electrostatic parameter space pointing out where interface state effects exceed space-charge effects and vice versa. This is done by introducing another treatment of the electrostatic problem. We also find that the image force effect on the barrier height due to the insertion of a material with lower dielectric constant than the semiconductor in between the Schottky contact is small but *positive*. This is in contrast to what might be expected from effective-medium theory. We conclude with an examination of ballistic electron emission microscopy results of pentacene modified Au/*n*-Si(111) Schottky diodes as a case study. Using the tools fore mentioned, we infer the *local* charge neutrality level and density of interface gap states (to an area of 500×500 nm^2) from barrier height statistics and pentacene monolayer heights.

DOI: 10.1103/PhysRevB.79.165313 PACS number(s): 73.30.+y, 77.55.+f, 73.20.−r, 73.40.−c

I. INTRODUCTION

There has been much interest of late in the modification of interface physics with molecular layers. Recent efforts include the use of molecular layers[1] or thin organic films[2] in the construction of hybrid organic-inorganic devices and attempts to elucidate transport mechanisms across these modified interfaces.[3] One approach to examining the effects of these layers on interface physics is modifying well-known junctions by adding organic layers in between and measuring the changes in the junction characteristics. The Schottky contact is one such example. Several studies[2,4–9] show that the addition of these films changes the barrier heights observed. However, some of the mechanisms responsible for these remain unclear. For instance, Kampen and co-workers[2] attributed the barrier lowering he observed to image force effects while others[4,5] observed changes in the space-charge region. The variety of molecules, preparation methods, and substrates used occlude the interface physics. In particular, the use of macroscopic measurement techniques such as current-voltage and capacitance-voltage (*I*-*V* and *C*-*V*) makes it hard to directly pinpoint the interface physics that results from the addition of organic layers which tend to be inhomogeneous. Here we make some effort to address these.

Electrostatic effects and modified barrier heights have a sixty year history. Bardeen[10] first proposed interface states and their corresponding surface-state charges to account for the insensitivity of Schottky barrier heights to metal work functions known as Fermi-level pinning. Others[11–13] further elaborated on this. In particular, Cowley and Sze[13] provided the standard framework[13,14] for addressing these effects in the context of Fermi-level pinning. This framework is certainly applicable in the case of organic-modified Schottky contacts.

Here, we seek to clarify some electrostatic concepts[13] in the context of organic thin films added in between a Schottky contact. One salient point is the set of parameters that make the interface gap states effect dominant. We address this by approaching the calculation differently and are able to derive a form more amenable to analysis. We work out analytically the parameter space in terms of the interface states and space-charge contributions to the barrier height change. We draw the parameter space out in terms of the charge neutrality level, doping density, density of interface states, dielectric thickness, and dielectric constant. We also clarify some confusion in the literature[2] associated with the image force effect due to a thin organic layer inserted between the metal and semiconductor. Finally, we use ballistic electron emission microscopy (BEEM) results of pentacene modified Au/*n*-Si(111) Schottky contacts as a case study to illustrate the local effects[15] of the pentacene which cannot be discerned using other techniques. These results allow us to infer the charge neutrality level and density of interface states locally.

II. ELECTROSTATIC EFFECTS

We consider the case of a thin organic film or indeed any dielectric thin film transparent to electrons having energies higher than the Schottky barrier height.[13] As such, we can assume that the electrochemical energies at the metal/thin organic film/semiconductor heterojunction line up.[16] Here, the thin organic film is treated as a dielectric layer with a dielectric constant ϵ_{org}. This allows us to write down the following relation for the metal work function:

$$\phi_m = \Delta + \chi + \psi_n + \xi_n, \tag{1}$$

where Δ is the potential drop across the organic layer, χ is the semiconductor electron affinity, ψ_n is the potential difference between the bulk semiconductor and the surface of the semiconductor, and ξ_n is the conduction-band offset (from the semiconductor Fermi level) as defined in Fig. 1. Since ϕ_m, χ, and ξ_n are material constants, we observe that

$$\Delta + \psi_n = \mathrm{const} = \psi_{bi}. \tag{2}$$

Using Eq. (2), we can work out the partition of the potential drop across the organic layer Δ and the potential drop across

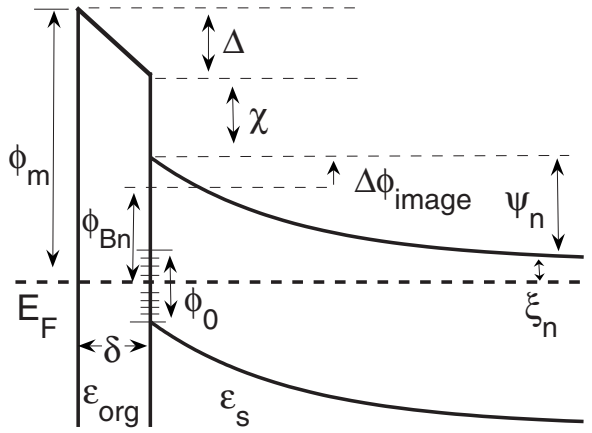

FIG. 1. Band diagram of the metal/dielectric/semiconductor heterojunction. The arrow for the image force effect $\Delta\phi_{\text{image}}$ indicates its direction convention.

the semiconductor layer ψ_n. In our case, we take $\Delta=\Delta_{\text{org}}^{\text{space}}+\Delta_{\text{org}}^{\text{int}}$ which are the space-charge and interface gap states contributions, respectively.

A. Interface states and space charge

The contributions to the total potential drop are as follows. The contribution of the space charge to the potential drop (using the depletion approximation) in the organic layer is[14]

$$\Delta_{\text{org}}^{\text{space}}=\frac{eN\delta}{\epsilon_{\text{org}}}W_n=\frac{1}{\epsilon_{\text{org}}}\sqrt{2e\epsilon_s N\delta^2(\psi_n-kT/e)}. \tag{3}$$

δ is the thickness of the organic layer, ϵ_s is the semiconductor dielectric constant, W_n is the depletion width in the semiconductor (which changes with the addition of the dielectric layer), and N is the doping density of the semiconductor. This expresses the space-charge contribution as a function of the potential drop in the semiconductor ψ_n.

We can also write down the contribution to the potential drop across the organic film arising from the interface gap states. This can be written by considering the charge neutrality level[10,13,14] as

$$\Delta_{\text{org}}^{\text{int}}=-\frac{eD_{it}\delta(E_g-e\phi_0-e\psi_n-e\xi_n)}{\epsilon_{\text{org}}}, \tag{4}$$

where D_{it} is the density of interface gap states and E_g is the band gap and ϕ_0 is the charge neutral level. Using Eq. (2), we can write down the following:

$$\psi_n+\Delta_{\text{org}}^{\text{int}}+\Delta_{\text{org}}^{\text{space}}=\text{const}=\psi_{bi}. \tag{5}$$

This tells us that the equilibrium condition (as measured by the Schottky barrier height) is given by balancing the contributions to the total potential drop which remains invariant. It is the sum of the space charge, interface gap states terms, and the potential drop in the semiconductor that give the resultant ψ_n. To simplify the notation, we introduce the following quantities:

$$y=\sqrt{\psi_n-kT/e}, \tag{6}$$

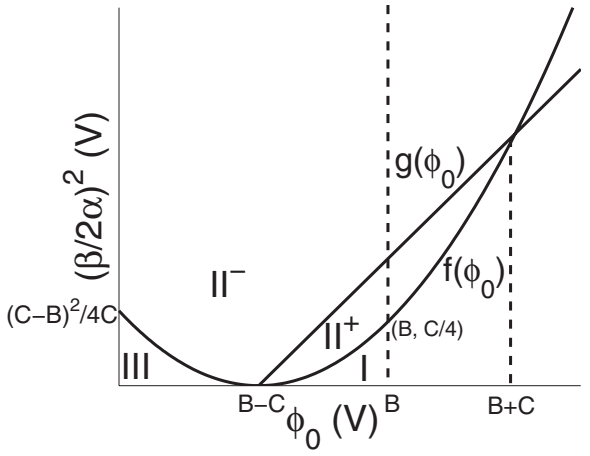

FIG. 2. Schematic of the parameter space for the combined space-charge and interface states effects considered in Eqs. (11) and (13). A derivation of this sketch is presented in the Appendix. $f(\phi_0)=\frac{(C-B+\phi_0)^2}{4C}$ and $g(\phi_0)=\frac{\phi_0+C-B}{2}$ and $B=E_g/e-\xi_n-kT/e$ and $C=\psi_{bi}-kT/e$. Regimes I and II exhibit barrier height lowering and regime III exhibits barrier height raising (more details in the text). We note that the y axis $(\beta/2\alpha)^2$ is independent of δ and ϵ_{org} and $(\beta/2\alpha)^2\propto N/D_{it}^2$. It is useful to note that the critical point (necessary condition) differentiating barrier lowering and raising behavior is $B-C=E_g/e-(\phi_m-\chi)$.

$$\alpha=\frac{e^2D_{it}\delta}{\epsilon_{\text{org}}}, \tag{7}$$

$$\beta=\frac{\delta\sqrt{2e\epsilon_s N}}{\epsilon_{\text{org}}}, \tag{8}$$

$$\nu=\alpha(E_g/e-\xi_n-\phi_0-kT/e). \tag{9}$$

It is useful to note that α is dimensionless and β has dimensions of $V^{1/2}$. α and β characterize the strength of the interface gap states and space-charge contributions, respectively. Equation (5) simplifies to a quadratic equation in y,

$$(\alpha+1)y^2+\beta y-\nu-\psi_{bi}+kT/e=0. \tag{10}$$

The solution to this (taking only the positive root as $\sqrt{\psi_n-kT/e}\geq 0$) is

$$y=\frac{-\beta+\sqrt{\beta^2+4(\alpha+1)(\nu+\psi_{bi}-kT/e)}}{2(\alpha+1)}. \tag{11}$$

We note that the barrier height is simply

$$\phi_{Bn}=\psi_n+\xi_n+\Delta\phi_{\text{image}}, \tag{12}$$

where $\Delta\phi_{\text{image}}$ is the total image potential effect. A discussion of $\Delta\phi_{\text{image}}$ in the context of a dielectric interfacial layer is presented in Sec. II B. Using Eqs. (6) and (12), the corresponding Schottky barrier height is

$$\phi_{Bn}=\psi_n+\xi_n+\Delta\phi_{\text{image}}=y^2+kT/e+\xi_n+\Delta\phi_{\text{image}}. \tag{13}$$

Though expressed in a different form, this produces the same result as Ref. 13 if $\phi_m-\chi$ in Ref. 13 is replaced with

$\psi_{bi}+\xi_n$ [from Eq. (1)]. Using our derivation (in contrast to Ref. 13), we can describe analytically the parameter space of the combined effect which to our knowledge has not been addressed before. We show a schematic in Fig. 2. This depicts the various regimes for finite $\frac{\delta}{\epsilon_{org}}$ where changing the charge neutrality level ϕ_0 or the ratio between β and α (β/α gives the relative strengths of the space-charge effect to the interface gap states effect) alters the behavior of the system. These regimes (derived in the Appendix) are

(I) Barrier height will be lowered with finite δ. In this regime, Δ_{org}^{int} is always positive. $\Delta_{org}^{int} > \Delta_{org}^{space}$ with small δ but there exists a finite δ [Eq. (14)] for which $\Delta_{org}^{space} > \Delta_{org}^{int}$.

(II) Barrier height will be lowered with finite δ. $\Delta_{org}^{space} > |\Delta_{org}^{int}|$ for all finite δ.

(III) Barrier height will increase. Here $|\Delta_{org}^{int}| > \Delta_{org}^{space}$ for all finite δ. In this regime, Δ_{org}^{int} is always negative.

In regime I, the barrier height is always lowered with finite δ but the region where the interface states dominates (and hence the region where just the interface states contribution to the barrier lowering can be considered alone as in Ref. 13) has an upper bound. Beyond a critical δ [as in Eq. (14)], the space-charge effect becomes larger than the interface states effect such that $\Delta_{org}^{space} > \Delta_{org}^{int}$. This δ is given by

$$\frac{\delta}{\epsilon_{org}^{r}} > \epsilon_0 \left(\frac{\psi_{bi} - kT/e - \gamma_+^2}{\lambda} \right) = \left(\frac{\delta}{\epsilon_{org}^{r}} \right)^{critical}, \qquad (14)$$

where γ_+ and λ are as defined in the Appendix. ϵ_{org}^{r} is the relative dielectric constant of the organic, such that $\epsilon_{org}^{r}\epsilon_0 = \epsilon_{org}$. We find that λ is always positive (see the Appendix). In this regime $\psi_{bi} - kT/e - \gamma_+^2 > 0$. This means that there always exists a δ for which $\Delta_{org}^{space} > \Delta_{org}^{int}$. The caveat here is that this δ may be far too large, such that the thin dielectric assumption which allows the electrochemical energy to equilibrate throughout is violated.[16] We note that the right-hand side is independent of ϵ_{org}^{r}.This allows us some intuition to the problem. If interface states dominate the lowering with a particular set of parameters, increasing $\delta/\epsilon_{org}^{r}$ (either by increasing the thickness or lowering the dielectric constant of the dielectric layer) will increase the space-charge contribution to the potential drop across the thin organic film. It is also helpful to note that in this regime, both space charge and interface states contribute a positive potential drop to Δ and lower the barrier.

The $(\delta/\epsilon_{org}^{r})^{critical}$ is plotted in Fig. 3. The $(\delta/\epsilon_{org}^{r})^{critical}$ decreases with increasing doping density N and increases with increasing density of interface gap states (red, black, and green curves) as expected. We also see that for $D_{it} = 10^{12}$ cm^{-2} eV^{-1}, there exist doping densities which make $(\delta/\epsilon_{org}^{r})^{critical}$ negative. This means that all finite δ (since $\delta > 0$) in that region will result in $\Delta_{org}^{space} > |\Delta_{org}^{int}|$. This is regime II. Increasing the doping density increases the ratio $(\beta/2\alpha)^2$ and allows for a crossover from regime I to regime II (see Fig. 2).

Regime II exhibits barrier height lowering where $\Delta_{org}^{space} > |\Delta_{org}^{int}|$ for all finite δ. Here, the interface states can cause a negative potential drop. However, since the space-charge effect is always greater, this is not discernable in the barrier modification alone. We note that the charge neutrality level ϕ_0 is practically bounded by the energy gap E_g/e.

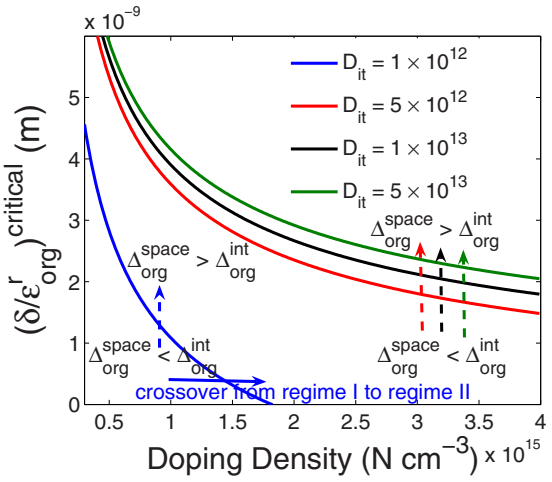

FIG. 3. (Color online) Plot of $(\delta/\epsilon_{org}^{r})^{critical}$ [the right-hand of Eq. (14)] showing the critical $\delta/\epsilon_{org}^{r}$ when $\Delta_{org}^{space} > \Delta_{org}^{int}$ at various densities of interface states D_{it} and doping densities N. The dotted arrows show the change from $\Delta_{org}^{space} < \Delta_{org}^{int}$ to $\Delta_{org}^{space} > \Delta_{org}^{int}$ by changing $\delta/\epsilon_{org}^{r}$ across the critical line. We note that all the doping densities shown given the density of interface states for the red, black, and green curves place the system in regime I. The doping densities, corresponding to the part of the blue curve that is above zero, place the system in regime I. The doping densities, corresponding to the blue curve when it dips below zero, place the system in regime II. Increasing the doping density (solid blue arrow) makes the system crossover from regime I to regime II.

Regime III exhibits barrier increase. Since the space-charge effect always accounts for a positive potential drop (and hence barrier lowering), all the barrier increase comes from the interface states. This effect occurs if $\phi_0 < B - C = E_g/e - \xi_n - \psi_{bi}$. Figure 2 shows a clear separation of necessary conditions for barrier height raising ($\phi_0 < B - C$) and barrier height lowering ($\phi_0 > B - C$) for regimes III and I, respectively.

The entire analysis presented above remains valid even with an interface dipole. The presence of an interface dipole merely shifts the relative energies by an amount equal to the magnitude of the interface dipole. Exceptionally, large interface dipoles (>1 eV) may swamp the effects discussed above.

B. Image force effect

We now clarify image force effects. Again we consider the thin organic film as a dielectric layer. The metal surface needs to be an equipotential and this results in an image potential (the dotted lines in Fig. 4) in the thin organic layer and the semiconductor. Since the image plane is the metal surface, the image force in the semiconductor is given by

$$F = -\frac{e^2}{4\pi\epsilon_s(2x + 2\delta)^2}, \quad x > 0, \qquad (15)$$

where x is measured from the semiconductor-organic layer interface and δ is the organic layer thickness. With the inter-

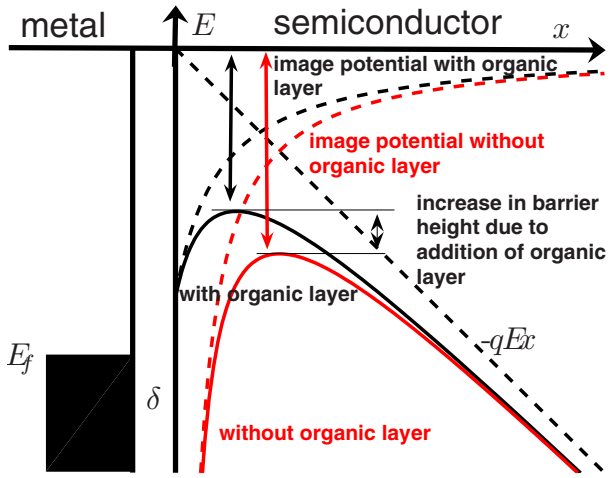

FIG. 4. (Color online) Energy diagram between metal-thin organic layer semiconductor showing barrier lowering (due to image force effects) for the case without the organic layer (red) and barrier lowering with the organic layer (black). Comparing the black and the red curves, we find that the effective barrier height is higher with the organic layer than without the organic layer, leading to an effective barrier raising. For simplicity and clarity, this sketch ignores the interface states and space-charge effects described in Sec. II A, which would change the interface electric field and the barrier height. However, we include a full treatment of these effects (coupled together) in all the other calculations and figures in this paper.

face electric field inside the semiconductor E_m, the potential energy (black solid line in Fig. 4) in the semiconductor becomes

$$\mathrm{PE} = -\frac{e^2}{16\pi\epsilon_s(x+\delta)} - e|E_m|x, \quad x > 0. \tag{16}$$

Solving this for the maximum potential point inside the semiconductor, we obtain x_m the distance the maxima is from the semiconductor-organic layer interface, as

$$x_m = \max\left[\sqrt{\frac{e}{16\pi\epsilon_s|E_m|}} - \delta, 0\right]. \tag{17}$$

The metal-semiconductor barrier occurs only in the semiconductor (and not in the organic layer). However, the turning point of Eq. (16) can occur inside the organic layer. If this occurs, the appropriate x_m to take is $x_m=0$ since this point will now be the highest potential point in the semiconductor. The max function [in Eq. (17)] accounts for this. The image potential lowering is therefore

$$\Delta\phi_{\mathrm{image}} = -\frac{e}{16\pi\epsilon_s(x_m+\delta)} - |E_m|x_m. \tag{18}$$

This reduces to the usual formula[14] for $\delta=0$. It is hard to picture the contribution of $\Delta\phi_{\mathrm{image}}$ to the total barrier height modification because the barrier heights and the interface electric fields can change due to the potential drop Δ across the thin organic layer. We plot (Fig. 4) the case where neither of these changes to illustrate the nonintuitive effect that the addition of the thin organic layer has. Here, keeping the interface electric field and the initial barrier height constant, we see that the addition of an organic layer effectively *increases* the barrier height from the case without the organic layer. We use this to emphasize that the primary image force effect *due* to the *addition* of the interfacial layer is the moving back of the image plane. This is in contrast to a naïve application of effective-medium theory which leads to the erroneous conclusion that the image force effect due to the addition of an interfacial layer decreases the barrier height.[2] We note that the dielectric constant of the organic film only enters indirectly through other effects (such as the interface gaps states and space-charge effects) that change the interface electric field. We hope that this clarifies some of the confusion in the literature[2] about the use of image force formulae.

III. DISCUSSION

It is expected that for most systems, the interface states effect should dominate. $(\beta/2\alpha)^2$ for the parameters used[17] is on the order of 10^{-6}, which is very close to the abscissa of Fig. 2 relative to the voltage scales set by B and C. For space-charge effects to be a dominant effect, a very high doping density or low interface states density is needed. Also, the transition from interface gap states dominated to space charge dominated in regime I illustrated in Fig. 3 is only practical if the δ used is small enough for the assumption that the electrochemical energies of the metal and semiconductor line up is valid. This is probably only practically observable in samples with very low interface states density (such as the blue curve in Fig. 3 or lower). Image force effects are negligible (we will see this in Fig. 7) when an interfacial layer is inserted between the metal/semiconductor interface and do not account for the lowering in barrier height as previously suggested.[2,9] It is likely that the interface gap states or space-charge effects are responsible for the lowering observed in Ref. 2.

There is a lack of resolution in many of the studies on the effects of thin organic films on Schottky contacts. These studies rely mainly on macroscopic techniques such as current-voltage and capacitance-voltage measurements. Some relevant concerns are (i) incomplete and nonuniform coverage of the organic layer in the heterojunction, and (ii) the effect of boundaries of the diodes when these measurements are performed. Because these methods take the average over the entire sample, it is difficult to deconvolute the various contributions to the interface measurements.

BEEM and ballistic electron emission spectroscopy (BEES),[18–20] on the other hand, allow for the nanoscale characterization of interfaces. BEEM is a three-terminal scanning tunneling microscope (STM) technique which injects hot electrons into a thin metal layer above the metal/semiconductor interface. These electrons travel to the interface and those with energy higher than the local Schottky barrier height (and obeying momentum conservation rules) are allowed to pass into the semiconductor. A collector current $I_{\mathrm{collector}}$ at the semiconductor allows one to study the interface. BEEM enables the imaging of the metal/semiconductor interface with nanometer resolution and thus allows the measurement of local Schottky barrier heights and

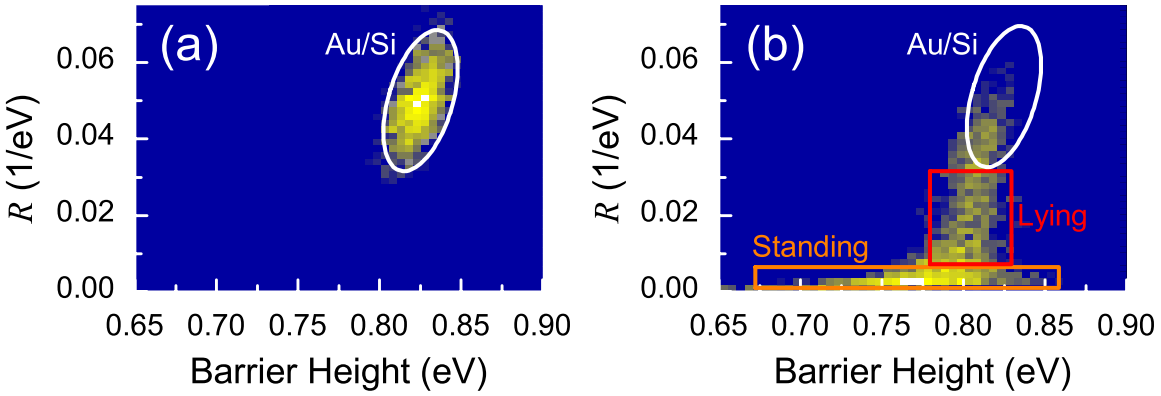

FIG. 5. (Color online) Statistical dual-parameter plot of the transmission factor R and barrier height ϕ_B. Histograms of ϕ_B and R for (a) Au/n-Si(111) and (b) Au/pentacene/n-Si(111) obtained from 3372 and 5296 BEES spectra, respectively. These were combined in the density plots (dual parameter) seen above where the intensity indicates normalized counts. The large spread in the box (orange) for the standing pentacene is due to the low signal-to-noise ratio. This gave a larger spread in the barrier heights fitted. We, however, find a systematic decrease in the average barrier height. We identify the average barrier height for Au/n-Si(111) as 0.83 eV, Au/lying pentacene/n-Si(111) as 0.8eV, and Au/standing pentacene/n-Si(111) as 0.76eV. The statistical samples shown are taken from 500×500 nm^2 areas within each device.

the elucidation of Schottky barrier inhomogeneity. Sweeping the STM tip voltage (BEES) and measuring the collector current also allow us to infer the barrier height of the metal-semiconductor interface without applying a bias directly to the sample. The BEEM current follows the power law:[20]

$$\frac{I_{\mathrm{BEEM}}}{I_{\mathrm{tunnel}}} = R\frac{(eV-\phi_B)^2}{eV}, \tag{19}$$

where V is the applied tip voltage. The BEES curves can be fitted to obtain the barrier height ϕ_B and the transmission R to characterize the interface.

We consider a BEEM study of Au/n-Si(111) diodes and pentacene modified Au/n-Si(111) diodes.[9] In the pentacene-modified sample, pentacene was deposited on an H-terminated n-Si(111) surface by sublimation at a temperature of $\sim$200 °C and chamber pressure of $\sim 5 \times 10^{-5}$ Pa. In order to prepare both Au/pentacene/n-Si(111) and reference Au/n-Si(111) diodes on the same substrate, a shadow mask technique was used. The samples were transferred into a high-vacuum Au evaporator, where $\sim$15 nm of Au was deposited onto either the H-terminated n-Si(111) or the pentacene/n-Si(111) region through another shadow mask which defined Au electrodes of 0.5 mm in diameter. This procedure allowed the preparation of Au/pentacene/n-Si(111) and Au/n-Si(111) devices on the same sample for direct comparison. The doping density of the n-Si was 10^{15} cm^{-3}. More experimental details are available in Ref. 9.

Using BEEM, we were able to image the buried pentacene islands at the interface.[9] Here we identified regions with no coverage, with islands of lying down molecules and islands of standing up molecules and with islands that were more than one monolayer. This is evidence of nonuniform and incomplete coverage. We made a statistical analysis of the BEES fit to Eq. (19). These were plotted in a dual-parameter plot of the transmission factor R against the barrier height ϕ_B, with the number of samples in a particular bin as the intensity (Fig. 5). The advantage of this representation is that it allows for a correlation between transmission and barrier height to be seen easily.

There is a correlation between lower barrier heights and lower transmission in the pentacene-modified diodes. Comparing this with the unmodified Au/n-Si(111), a systematic modification of the transmission and barrier height statistics can be discerned. The lowest transmissions (orange box in Fig. 5) can be attributed to the thicker upright pentacene where the greater barrier modification (in this case lowering)

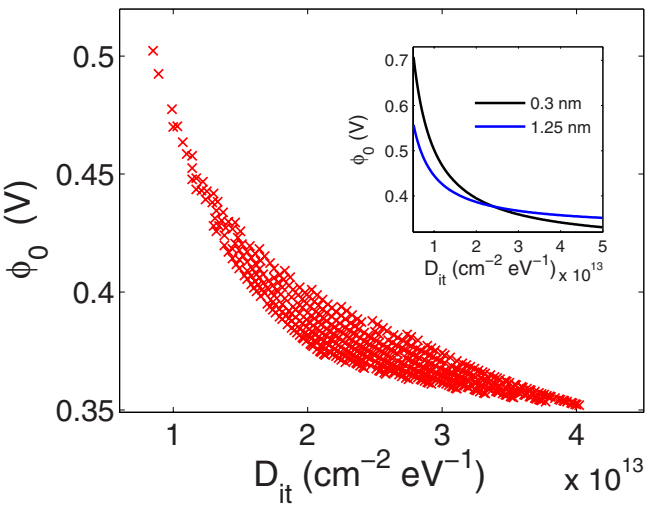

FIG. 6. (Color online) D_{it} and ϕ_0 inferred from pentacene heights and barrier lowering (0.8 and 0.76 V from the averages in Fig. 5) that satisfied Eq. (13). The values of pentacene heights used were $\delta_{\mathrm{lying}} = (0.30 \pm 0.05)$ nm and $\delta_{\mathrm{standing}} = (1.25 \pm 0.25)$ nm. (Inset) Graph of the D_{it} and ϕ_0 that satisfy the barrier lowering observed for a specific $\delta_{\mathrm{lying}} = 0.3$ nm and $\delta_{\mathrm{standing}} = 1.25$ nm in Eq. (13) (Ref. 17). Their intersection indicates the D_{it} and ϕ_0 inferred from the data of the specific heights used and lowered barriers. Each point in the larger panel is derived from intersections of two curves, from two pentacene heights, such as the inset.

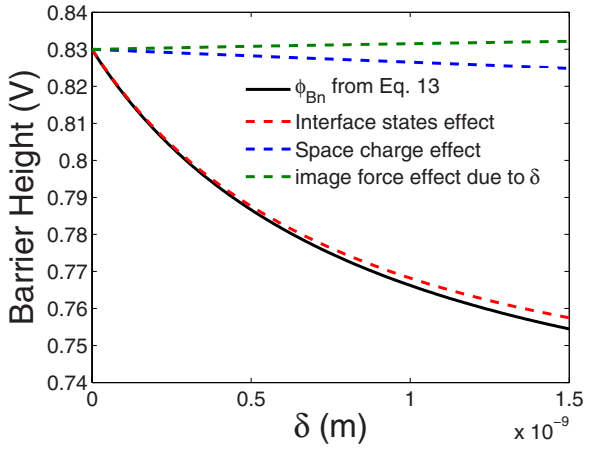

FIG. 7. (Color online) Contributions of the space-charge, interface states, and image force effects plotted individually. Here, we use the parameters derived previously of $D_{it}=2.4\times10^{13}$ cm^{-2} and $\phi_0=0.38$ V. As before, we use $N=10^{15}$ cm^{-3}. We start with the Au/*n*-Si(111) barrier height measured in Fig. 5.

can be expected. The lowered transmissions (red box in Fig. 5) can be correlated with the lying pentacene which resulted in barrier lowering though not as much as the standing pentacene. It is clear that the varying thicknesses (standing and lying pentacene) alter the local barrier height differently. Macroscopic techniques such as *C-V* and *I-V* cannot discern this.

In the light of the tools developed in Secs. II A and II B, we re-examine the data[9] to include interface gap states, space-charge effects, as well as image force effects. In fact using common values of N and D_{it}, we expect (see Fig. 2) that the interface states contribution should dominate the lowering.

We can identify the barrier lowering (Fig. 5) to be Au/lying pentacene/*n*-Si(111) as 0.8 eV and Au/standing pentacene/*n*-Si(111) as 0.76 eV. This corresponds to lying down pentacene heights of $\delta=(0.30\pm0.05)$ nm and standing pentacene heights of $\delta=(1.25\pm0.25)$ nm.[9,15] Using Eq. (13), the heights of the lying down and standing pentacene[9,15] together with the measured average lowered barrier heights allow us to determine the density of interface gap states D_{it} and the charge neutrality level ϕ_0. We do this by plotting D_{it} and ϕ_0 (inset of Fig. 6) that satisfy Eq. (13) for the barrier height lowering observed for a particular thickness. For example (see inset of Fig. 6), we plot D_{it} and ϕ_0 that satisfy the barrier height lowering of the lying pentacene to 0.8 eV with a thickness of 0.3 nm in the blue curve. We repeat this for the standing pentacene for a height of 1.25 nm and lowered barrier height of 0.76 eV in the black curve. Their intersection gives the ϕ_0 and D_{it} inferred from these two values. This can be repeated for all the possible combinations of thicknesses within the error bars above (main panel of Fig. 6).

The plotted points (Fig. 6) allow us to discern $D_{it}=(2.4\pm0.7)\times10^{13}$ cm^{-2} eV^{-1} and $\phi_0=(0.38\pm0.02)$ V. This is within the range of experimentally determined values of density of interface states and charge neutrality level for silicon.[13] We note, however, that the error bars we have for the charge neutrality level are significantly smaller (about 1 order of magnitude) than those of Ref. 13. Tersoff's[21] theoretically derived the charge neutrality level for silicon of $\phi_0^{\text{Tersoff}}=0.36$ V is also within the error bars of our determined charge neutrality level. We note that the statistical dual-parameter plot was drawn from BEES measurements in a 500×500 nm^2 area. This is contrasted with diode sizes of ~100 μm diameter that typical *C-V* measurements are carried out on.

With these values we can compare the magnitudes of the contributions (interface gap states, space-charge, and image force effects) to the observed barrier height lowering. Using Eq. (13) we plot the contributions in Fig. 7. Here we see that the main contribution to the barrier height lowering comes from the interface states (red dotted lines). The space-charge and image force effects are not significant. Most nonintuitive is the image force contribution being positive as illustrated in Figs. 4 and 7. Coming full circle, we can check that for the parameters used, our system falls in regime I of Fig. 2, where the interface states effect dominates for small $\delta/\epsilon_{\text{org}}$.

IV. CONCLUSION

We have elaborated on interface states, space-charge, and image force effects in the context of thin organic films modifying Schottky barrier heights. We have also derived the different regimes that arise from considering interface states and space-charge effects together showing the parameter space of the effects. We have found that the image force effects due to an interfacial layer of an organic thin film added to modify the Schottky barrier are small and *positive* contrary to what might be expected. This clarifies the use of image force effects in the literature.[2]

We applied this to a BEEM study of pentacene-modified Au/*n*-Si(111) Schottky diodes and found that the effects described above could account for the barrier lowering. In particular, interface states dominated the barrier lowering. Using known heights of the pentacene islands (standing and lying down), we were able to identify the density of interface states and charge neutrality level *locally* (to an area 500×500 nm^2). These are comparable to the values expected for silicon surfaces. This further acts as corroborating evidence for attributing the decreased transmission to the standing and lying pentacene molecules. Quantitatively, analyzing the statistical dual-parameter plots is potentially useful for characterizing interfaces. This is illustrated by the increased spatial resolution (500×500 nm^2) and the significantly more precise value for the charge neutrality level.

The inhomogeneity of the barrier heights and transmission seen in our BEEM study underscores the nonuniform coverage of organic layers on Si surfaces and vindicates the need to use more local measurements to elucidate interface physics. In particular, the inferred local (to an area 500×500 nm^2) charge neutrality level and density of interface states yield microscopic information, once reliant on conventional macroscopic methods such as capacitance-voltage measurements, to elucidate interface properties.

ACKNOWLEDGMENT

We thank Bihui Li for a critical reading of this manuscript.

APPENDIX

Here we derive the condition for $\Delta_{\text{org}}^{\text{space}} > |\Delta_{\text{org}}^{\text{int}}|$. We can write down the contribution of the space charge as

$$\Delta_{\text{org}}^{\text{space}} = \beta y, \tag{A1}$$

and the contribution of the interface states as

$$\Delta_{\text{org}}^{\text{int}} = \alpha y^2 - \nu. \tag{A2}$$

Given usual parameters (for metal-semiconductor junctions), it is reasonable to assume that $\nu > 0$. We shall consider this case only. The critical point for $\Delta_{\text{org}}^{\text{space}} > |\Delta_{\text{org}}^{\text{int}}|$ occurs at the positive roots of

$$|\alpha y^2 - \nu| - \beta y = 0. \tag{A3}$$

One positive root is

$$\gamma_+ = \frac{\beta + \sqrt{\beta^2 + 4\alpha\nu}}{2\alpha}. \tag{A4}$$

The other critical point is

$$\gamma_- = \frac{-\beta + \sqrt{\beta^2 + 4\alpha\nu}}{2\alpha}. \tag{A5}$$

We note that in both cases, $\gamma_\pm$ are independent of δ and ϵ_{org} [also see Eq. (A8)]. Since we are solving for a condition for δ, this helps greatly because we can treat this as a constant in our manipulation. In the first case, γ_+, the condition for $\Delta_{\text{org}}^{\text{space}} > |\Delta_{\text{org}}^{\text{int}}|$ reduces to $y < \gamma_+$. This is

$$\frac{-\beta + \sqrt{\beta^2 + 4(\alpha+1)(\nu + \psi_{bi} - kT/e)}}{2(\alpha+1)} < \gamma_+. \tag{A6}$$

After some manipulation, we get

$$\psi_{bi} - kT/e - \gamma_+^2 < \alpha\gamma_+^2 - \nu + \beta\gamma_+. \tag{A7}$$

We observe that the right-hand side is linear in δ. By redefining the variables as

$$\beta_0 \frac{\delta}{\epsilon_{\text{org}}} = \beta, \quad \alpha_0 \frac{\delta}{\epsilon_{\text{org}}} = \alpha, \quad \nu_0 \frac{\delta}{\epsilon_{\text{org}}} = \nu, \tag{A8}$$

$$\lambda = \alpha_0\gamma_+^2 - \nu_0 + \beta_0\gamma_+, \tag{A9}$$

we can write

$$\psi_{bi} - kT/e - \gamma_+^2 < \lambda \frac{\delta}{\epsilon_{\text{org}}}. \tag{A10}$$

This gives the condition in Eq. (14). We find that $\lambda > 0$ for all nonzero D_{int} and N. If $\psi_{bi} - kT/e - \gamma_+^2 > 0$, this means that there is a critical δ after which space-charge effects will become larger than interface state effects. If $\psi_{bi} - kT/e - \gamma_+^2 < 0$, this means that the critical δ is negative. However, since δ is always positive this means that for all finite δ, space-charge effects will be larger than interface states effects.

We now consider the second case $\Delta_{\text{org}}^{\text{space}} > |\Delta_{\text{org}}^{\text{int}}|$ when $y > \gamma_-$. After manipulation, we obtain a similar expression as before

$$\psi_{bi} - kT/e - \gamma_-^2 > \frac{\delta}{\epsilon_{\text{org}}}\{\alpha_0\gamma_-^2 - \nu_0 + \beta_0\gamma_-\}. \tag{A11}$$

However, we find that the term in the brackets { } is zero. If $\psi_{bi} - kT/e - \gamma_-^2 > 0$, this merely demands that δ is finite. Put the other way round, there is no δ [after the first condition in Eq. (14)] such that interface effects would again dominate. This makes the condition in Eq. (14) a clean one where the division between $\Delta_{\text{org}}^{\text{space}} > |\Delta_{\text{org}}^{\text{int}}|$ and $|\Delta_{\text{org}}^{\text{int}}| > \Delta_{\text{org}}^{\text{space}}$ occurs across one line defined by Eq. (14). If $\psi_{bi} - kT/e - \gamma_-^2 < 0$, this means that for all finite δ, $|\Delta_{\text{org}}^{\text{int}}| > \Delta_{\text{org}}^{\text{space}}$. Recalling the quadratic expression for the interface states effects, this region corresponds to the negative contribution of $\Delta_{\text{org}}^{\text{int}}$.

We can identify regions which correspond to the changing signs of the two conditions. They are

(I) $\gamma_+^2 < \psi_{bi} - kT/e$. This gives $\Delta_{\text{org}}^{\text{int}} > 0$ and allows for the crossover detailed in Eq. (14).

(II) $\gamma_-^2 < \psi_{bi} - kT/e < \gamma_+^2$. This gives $\Delta_{\text{org}}^{\text{space}} > |\Delta_{\text{org}}^{\text{int}}| \forall$ nonzero δ.

(III) $\gamma_-^2 > \psi_{bi} - kT/e$. This gives $|\Delta_{\text{org}}^{\text{int}}| > \Delta_{\text{org}}^{\text{space}}$ and $\Delta_{\text{org}}^{\text{int}} < 0 \forall$ nonzero δ.

It useful to express these conditions in terms of regions in the parameter space of charge neutrality level ϕ_0 and the relative strengths of the space-charge and interface gap states effects $\beta/2\alpha$. So rewriting the conditions, we get

(I) $(\frac{\beta}{2\alpha})^2 < f(\phi_0)$ and $(\frac{\beta}{2\alpha})^2 < g(\phi_0)$,

(II$^+$) $(\frac{\beta}{2\alpha})^2 > f(\phi_0)$ and $(\frac{\beta}{2\alpha})^2 < g(\phi_0)$,

(II$^-$) $(\frac{\beta}{2\alpha})^2 > f(\phi_0)$ and $(\frac{\beta}{2\alpha})^2 > g(\phi_0)$, and

(III) $(\frac{\beta}{2\alpha})^2 < f(\phi_0)$ and $(\frac{\beta}{2\alpha})^2 > g(\phi_0)$, where $f(\phi_0) = \frac{(C-B+\phi_0)^2}{4C}$ and $g(\phi_0) = \frac{\phi_0 + C - B}{2}$ and $B = E_g/e - \xi_n - kT/e$ and $C = \psi_{bi} - kT/e$.

Using these, we can draw out the regions where space-charge or interface states effects are greater in Fig. 2. We note that these conditions are independent of δ and ϵ_{org}. It can be shown that the x intercept of $g(\phi_0)$ and the minimum of $f(\phi_0)$ both occur at $B - C$. We note that ϕ_0 is practically bounded by E_g/e, otherwise ϕ_0 would be in the conduction band.

*kejgoh@yahoo.com

[1] C. R. Kagan, D. B. Mitzi, and C. D. Dimitrakopoulos, Science **286**, 945 (1999).

[2] D. R. T. Zahn, S. Park, and T. U. Kampen, Vacuum **67**, 101 (2002); T. U. Kampen, S. Park, and D. R. Zahn, J. Vac. Sci. Technol. B **21**, 879 (2003); T. Kampen, A. Bekkali, I. Thurzo, D. R. T. Zahn, A. Bolognesi, T. Ziller, A. Di Carlo, and P. Lugli, Appl. Surf. Sci. **234**, 313 (2004).

[3] A. Bannani, C. Bobisch, and R. Möller, Science **315**, 1824 (2007).

[4] A. Türüt, N. Yalçin, and M. Saglam, Solid-State Electron. **35**, 835 (1992); Y. Onganer, M. Sağlam, A. Türüt, H. Efeoğlu, and S

Tüzemen, *ibid.* **39**, 677 (1996); Ö. Güllü, Ö. Bariş, M. Biber, and A. Türüt, Appl. Surf. Sci. **254**, 3039 (2008).
[5] A. R. Vearey-Roberts and D. A. Evans, Appl. Phys. Lett. **86**, 072105 (2005).
[6] H. Haick, M. Ambrico, T. Ligonzo and D. Cahen, Adv. Mater. (Weinheim, Ger.) **16**, 2145 (2004).
[7] M. A. Kuikka, W. Li, K. L. Kavanagh, and H.-Z. Yu, J. Phys. Chem. C **112**, 9081 (2008).
[8] S. Özcan, J. Smoliner, M. Andrews, and G. Strasser, T. Dienel, R. Franke, and T. Fritz, Appl. Phys. Lett. **90**, 092107 (2007).
[9] Kuan Eng J. Goh, A. Bannani, and C. Troadec, Nanotechnology **19**, 445718 (2008).
[10] J. Bardeen, Phys. Rev. **71**, 717 (1947).
[11] V. Heine, Phys. Rev. **138**, A1689 (1965).
[12] W. E. Spicer, P. W. Chye, P. R. Skeath, C. Y. Su, and I. Lindau, J. Vac. Sci. Technol. **16**, 1422 (1979).
[13] A. M. Cowley and S. M. Sze, J. Appl. Phys. **36**, 3212 (1965).
[14] S. M. Sze and Kwok K. Ng, *Physics of Semiconductor Devices*, 3rd ed. (Wiley, New York, 2007).
[15] T. Shimada, H. Nogawa, T. Hasegawa, R. Okada, H. Ichikawa, K. Ueno, and K. Saiki, Appl. Phys. Lett. **87**, 061917 (2005).
[16] The condition for the thickness of the dielectric film for which the electrochemical energies in the heterojunction can still line up is in practice a difficult one to write down. Here we consider the case where no bias is applied across the device (as is the case in BEES). The condition is connected to the practical time scales that samples are prepared and then measured. We can estimate (order of magnitude) the time taken to equilibrate as $\tau \propto e^{A\psi^{1/2}m_r^{1/2}\delta}$, where $A=1.025$ Å^{-1} eV$^{-1/2}$, ψ is the potential barrier, and m_r is the relative effective mass in the dielectric. For the pentacene effective mass of $m_r=0.3$, we find that 2 nm thickness takes just under 8 h to equilibrate. However, 4 nm takes more than 20 years. We emphasize that these are order of magnitude estimates.
[17] The values used in Eq. (13) were $\psi_{bi}=0.83$ V$-\xi_n-\Delta_{\text{image}}^{\delta=0}$, $\xi_n=0.3$ V, $kT/e=0.025$ V, $\epsilon_s^r=11.9$, and $\epsilon_{\text{org}}^r=4.0$. The value chosen for ψ_{bi} corresponds Au/n-Si(111) barrier measured. We can use this value for ψ_{bi} as a first-order approximation together with the thickness of the pentacene as δ. This makes the calculation cleaner as it is less dependant on measurements in the literature of $\phi_m-\chi$. We find that the higher-order corrections are significantly (a few orders of magnitude) smaller than the first-order approximation that we used.
[18] M. Prietsch, Phys. Rep. **253**, 163 (1995).
[19] W. J. Kaiser and L. D. Bell, Phys. Rev. Lett. **60**, 1406 (1988).
[20] L. D. Bell and W. J. Kaiser, Phys. Rev. Lett. **61**, 2368 (1988).
[21] J. Tersoff, Surf. Sci. **168**, 275 (1986).